Proceedings of the 8th International Conference on Structural Dynamics, EURODYN 2011
Leuven, Belgium, 4-6 July 2011
G. De Roeck, G. Degrande, G. Lombaert, G. Müller (eds.)
ISBN 978-90-760-1931-4

Passive-active vibration control for connected multi-building structures

Francisco Palacios-Quiñonero[1], Josep M. Rossell[1], José Rodellar[2], Raul Pons-López[3]
[1]Department of Applied Mathematics III, EPSEM-UPC, Av. Bases de Manresa 61-73, 08242-Manresa, Barcelona, SPAIN
[2]Department of Applied Mathematics III, ETSECCPB-UPC, Campus Nord, C2, 08034-Barcelona, SPAIN
[3]Mechanical Engineering senior student at EPSEM-UPC
email: francisco.palacios@upc.edu, josep.maria.rossell@upc.edu, jose.rodellar@upc.edu, raulponslopez@gmail.com

ABSTRACT: In this paper, a mixed passive-active control strategy to mitigate the seismic response of a three-building system is presented. The proposed strategy combines passive dampers, placed as inter-building linking elements, with local active control systems implemented in those buildings that require a higher level of seismic protection. Different active-passive control configurations are considered, which may be suitable for different levels of seismic protection and combine the high performance characteristics of active control systems with the simplicity, reliability, and low cost of passive control elements. The numerical simulations carried out to assess the performance of the proposed methodology indicate that the buildings vibrational response and the risk of inter-building pounding events may both be effectively mitigated by means of a proper active-passive control configuration.

KEY WORDS: Structural vibration control; Seismic mitigation; Connected control method; Multi-building structures.

1 INTRODUCTION

Structural Vibrational Control (SVC) for seismic mitigation is nowadays a well established field of research and engineering practice [5], [9]. Although the most appealing examples of SVC implementations are those involving huge structures as high towers or long-span bridges, it should be noted the existence of a large variety of medium-size and small-size strategic structures for which seismic protection may be of critical importance. Some clear examples are communication and command centers, emergency service facilities, hospitals, emergency power plants, etc. In all these cases, besides preventing structural failure and ensuring safety, the operational serviceability of the structure and equipment must also be assured. Moreover, despite the medium or small size of individual buildings, the overall system may be highly complex comprising two or more adjacent buildings and a variety of attached substructures, possibly requiring different levels of seismic protection.

When dealing with the seismic response of closely adjacent buildings, the possibility of inter-building collisions (pounding) should be considered. Pounding may cause severe structural damage, even collapse in some extreme situations [1]. Further, large acceleration pulses may result from the quick and massive pounding impacts, which can cause serious damage to building contents [6]. In recent years, the Connected Control Method (CCM) has proved to be an effective strategy to mitigate the building vibrational response and prevent inter-building pounding effects. In the CCM, adjacent buildings are linked together by means of coupling devices to provide appropriate reaction control forces. The application of the CCM using different kinds of passive, active, and semiactive linking devices has been investigated with positive results; some interesting references are [2], [3], [4], [7], [8], [10], [11].

The aim of this work is to explore the effectiveness of a mixed passive-active control strategy to mitigate the seismic response of a complex system consisting of three adjacent buildings. In the proposed strategy, a passive control system formed by a set of damping devices, which act as inter-building linking elements, is combined with one or more local active control systems implemented in those buildings that require a specially high level of seismic protection. As a result, a number of passive-active control configurations are obtained, which may be suitable for different levels of seismic protection and combine the high performance characteristics of the local active control systems with the simplicity, reliability, and low cost of the passive control elements.

The paper is organized as follows. In Section 2, a simplified dynamical model of the three-building coupled system is provided. In Section 3, the passive linking configurations are presented. Finally, in Section 4, the mixed passive-active control configurations are presented and discussed.

2 THREE-BUILDING CONNECTED SYSTEM

In this section, a simplified model for the three-building coupled system shown in Fig. 1 is presented. The buildings motion can be described by the second-order model

$$M\,\ddot{q}(t) + C\,\dot{q}(t) + K\,q(t) = T_u\,u(t) + T_w\,w(t), \qquad (1)$$

where M is the mass matrix; K and C are the total stiffness and damping matrices, respectively, including the stiffness and damping coefficients of the buildings $\mathcal{B}^{(j)}$ as well as the stiffness and damping coefficients of the linking systems $\mathcal{L}^{(j)}$; the vector of story displacements with respect to the ground is

$$q(t) = \left[q_1^1, q_2^1, q_3^1, q_1^2, q_2^2, q_3^2, q_4^2, q_5^2, q_1^3, q_2^3\right]^T, \qquad (2)$$

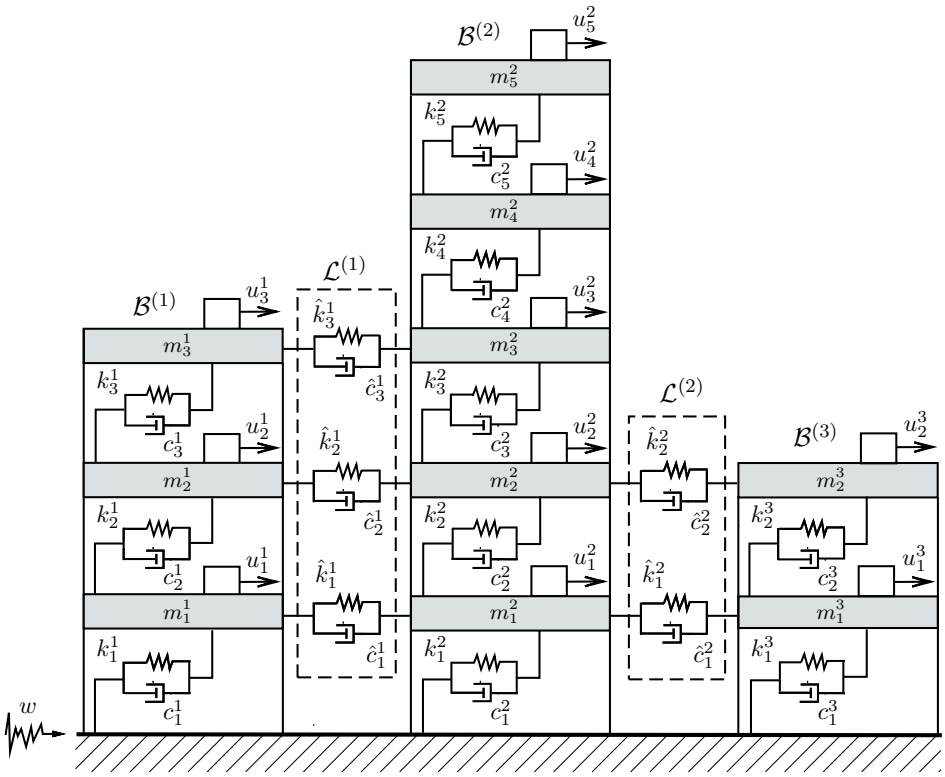

Figure 1. Three-building connected system

where q_i^j represents the displacement of the ith story in the jth building; the vector of control forces has a similar structure

$$u(t) = \left[u_1^1, u_2^1, u_3^1, u_1^2, u_2^2, u_3^2, u_4^2, u_5^2, u_1^3, u_2^3\right]^T, \tag{3}$$

T_u is the control location matrix; T_w is the disturbance input matrix, and $w(t)$ is the ground acceleration. Note that the explicit dependence on time has been omitted in (2) and (3) to simplify the notation; this will also be done in the sequel when convenient. The mass matrix in equation (1) has a block diagonal structure:

$$M = \begin{bmatrix} M^{(1)} & [0]_{3\times5} & [0]_{3\times2} \\ [0]_{5\times3} & M^{(2)} & [0]_{5\times2} \\ [0]_{2\times3} & [0]_{2\times5} & M^{(3)} \end{bmatrix},$$

where $[0]_{r\times s}$ is a $r\times s$ zero-matrix, and $M^{(j)}$ is the mass matrix of the jth building

$$M^{(1)} = \begin{bmatrix} m_1^1 & 0 & 0 \\ 0 & m_2^1 & 0 \\ 0 & 0 & m_3^1 \end{bmatrix}, \quad M^{(3)} = \begin{bmatrix} m_1^3 & 0 \\ 0 & m_2^3 \end{bmatrix},$$

$$M^{(2)} = \begin{bmatrix} m_1^2 & 0 & 0 & 0 & 0 \\ 0 & m_2^2 & 0 & 0 & 0 \\ 0 & 0 & m_3^2 & 0 & 0 \\ 0 & 0 & 0 & m_4^2 & 0 \\ 0 & 0 & 0 & 0 & m_5^2 \end{bmatrix}.$$

The total damping matrix may be written in the form

$$C = C_B + C_L,$$

where C_B is a block diagonal matrix corresponding to the internal damping of the buildings

$$C_B = \begin{bmatrix} C^{(1)} & [0]_{3\times5} & [0]_{3\times2} \\ [0]_{5\times3} & C^{(2)} & [0]_{5\times2} \\ [0]_{2\times3} & [0]_{2\times5} & C^{(3)} \end{bmatrix},$$

with tridiagonal blocks

$$C^{(1)} = \begin{bmatrix} c_1^1+c_2^1 & -c_2^1 & 0 \\ -c_2^1 & c_2^1+c_3^1 & -c_3^1 \\ 0 & -c_3^1 & c_3^1 \end{bmatrix}, \; C^{(3)} = \begin{bmatrix} c_1^3+c_2^3 & -c_2^3 \\ -c_2^3 & c_2^3 \end{bmatrix},$$

$$C^{(2)} = \begin{bmatrix} c_1^2+c_2^2 & -c_2^2 & 0 & 0 & 0 \\ -c_2^2 & c_2^2+c_3^2 & -c_3^2 & 0 & 0 \\ 0 & -c_3^2 & c_3^2+c_4^2 & -c_4^2 & 0 \\ 0 & 0 & -c_4^2 & c_4^2+c_5^2 & -c_5^2 \\ 0 & 0 & 0 & -c_5^2 & c_5^2 \end{bmatrix}, \tag{4}$$

and c_i^j denotes the damping coefficient of the ith story in the jth building. The matrix C_L corresponds to the linking systems and may be written as a block tridiagonal matrix

$$C_L = \begin{bmatrix} [\hat{C}^{(1)}]_{3\times3} & -[\hat{C}^{(1)}]_{3\times5} & [0]_{3\times2} \\ -[\hat{C}^{(1)}]_{5\times3} & [\hat{C}^{(1)}]_{5\times5}+[\hat{C}^{(2)}]_{5\times5} & -[\hat{C}^{(2)}]_{5\times2} \\ [0]_{2\times3} & -[\hat{C}^{(2)}]_{2\times5} & [\hat{C}^{(2)}]_{2\times2} \end{bmatrix},$$

where $\hat{C}^{(j)}$ is the damping matrix of the linking system $\mathcal{L}^{(j)}$

$$\hat{C}^{(1)} = \begin{bmatrix} \hat{c}_1^1 & 0 & 0 \\ 0 & \hat{c}_2^1 & 0 \\ 0 & 0 & \hat{c}_3^1 \end{bmatrix}, \; \hat{C}^{(2)} = \begin{bmatrix} \hat{c}_1^2 & 0 \\ 0 & \hat{c}_2^2 \end{bmatrix}, \tag{5}$$

$\hat{c}_i^j$ is the damping coefficient of the ith element in the jth linking system, and $[A]_{r\times s}$ denotes the *zero extension* of matrix A, which is a $r\times s$ matrix obtained from A by adding a proper number of ending zero-rows and zero-columns; for example, we have

$$[\hat{C}^{(1)}]_{5\times 5} = \begin{bmatrix} \hat{c}_1^1 & 0 & 0 & 0 & 0 \\ 0 & \hat{c}_2^1 & 0 & 0 & 0 \\ 0 & 0 & \hat{c}_3^1 & 0 & 0 \\ 0 & 0 & 0 & 0 & 0 \\ 0 & 0 & 0 & 0 & 0 \end{bmatrix}, \; [\hat{C}^{(2)}]_{5\times 2} = \begin{bmatrix} \hat{c}_1^2 & 0 \\ 0 & \hat{c}_2^2 \\ 0 & 0 \\ 0 & 0 \\ 0 & 0 \end{bmatrix}.$$

The total stiffness matrix may also be written in the form

$$K = K_B + K_L,$$

with

$$K_B = \begin{bmatrix} K^{(1)} & [0]_{3\times 5} & [0]_{3\times 2} \\ [0]_{5\times 3} & K^{(2)} & [0]_{5\times 2} \\ [0]_{2\times 3} & [0]_{2\times 5} & K^{(3)} \end{bmatrix},$$

and

$$K_L = \begin{bmatrix} [\hat{K}^{(1)}]_{3\times 3} & -[\hat{K}^{(1)}]_{3\times 5} & [0]_{3\times 2} \\ -[\hat{K}^{(1)}]_{5\times 3} & [\hat{K}^{(1)}]_{5\times 5} + [\hat{K}^{(2)}]_{5\times 5} & -[\hat{K}^{(2)}]_{5\times 2} \\ [0]_{2\times 3} & -[\hat{K}^{(2)}]_{2\times 5} & [\hat{K}^{(2)}]_{2\times 2} \end{bmatrix}.$$

The matrices $K^{(j)}$ and $\hat{K}^{(j)}$ can be obtained from (4), and (5), by replacing the damping coefficients c_i^j and $\hat{c}_i^j$ by the corresponding stiffness coefficients k_i^j and $\hat{k}_i^j$. The control location matrix T_u has the structure

$$T_u = \begin{bmatrix} T_u^{(1)} & [0]_{3\times 5} & [0]_{3\times 2} \\ [0]_{5\times 3} & T_u^{(2)} & [0]_{5\times 2} \\ [0]_{2\times 3} & [0]_{2\times 5} & T_u^{(3)} \end{bmatrix},$$

with $T_u^{(j)}$ denoting the control location matrix of the jth building. Finally, the disturbance input matrix, may be written in the form $T_w = -M\{\mathbf{1}\}_{10}$, where $\{\mathbf{1}\}_{10}$ is a column vector of dimension 10 with all its entries equal to 1.

From the second-order model (1), a first-order state-space model can be derived

$$\begin{cases} \dot{x}(t) = Ax(t) + Bu(t) + Ew(t), \\ y(t) = C_y x(t), \end{cases} \tag{6}$$

by taking the state vector

$$x(t) = \begin{bmatrix} q(t) \\ \dot{q}(t) \end{bmatrix}.$$

The state matrix in (6), has the structure

$$A = \begin{bmatrix} [0]_{10} & I_{10} \\ -M^{-1}K & -M^{-1}C \end{bmatrix},$$

where $[0]_r$ denotes a $r\times r$ zero-matrix, and I_r is the identity matrix of order r. The control and disturbance input matrices are, respectively,

$$B = \begin{bmatrix} [0]_{10} \\ M^{-1}T_u \end{bmatrix}, \quad E = \begin{bmatrix} [0]_{10\times 1} \\ -\{\mathbf{1}\}_{10} \end{bmatrix}. \tag{7}$$

Regarding to the output, different cases of interest may be considered. The vector of story displacements relative to the ground

$$y_d(t) = \left[q_1^1, q_2^1, q_3^1, q_1^2, q_2^2, q_3^2, q_4^2, q_5^2, q_1^3, q_2^3\right]^T,$$

can be obtained directly with the output matrix

$$C_{y_d} = \begin{bmatrix} I_{10} & [0]_{10} \end{bmatrix}.$$

The *inter-story drifts*, defined by

$$\begin{cases} \{y_s\}_1^j = q_1^j, \\ \{y_s\}_i^j = q_i^j - q_{i-1}^j, \quad 1 < i \le n_j, \end{cases}$$

represent the relative displacements between consecutive stories in the jth building, which has n_j stories. The vector of inter-story drifts

$$y_s(t) = \left[\{y_s\}_1^1, \{y_s\}_2^1, \{y_s\}_3^1, \{y_s\}_1^2, \{y_s\}_2^2, \{y_s\}_3^2, \{y_s\}_4^2, \{y_s\}_5^2, \{y_s\}_1^3, \{y_s\}_2^3\right]^T$$

can be obtained with the output matrix

$$C_{y_s} = \begin{bmatrix} C_{y_s}^{(1)} & [0]_{3\times 5} & [0]_{3\times 2} & [0]_{3\times 10} \\ [0]_{5\times 3} & C_{y_s}^{(2)} & [0]_{5\times 2} & [0]_{5\times 10} \\ [0]_{2\times 3} & [0]_{2\times 5} & C_{y_s}^{(3)} & [0]_{2\times 10} \end{bmatrix}, \tag{8}$$

where

$$C_{y_s}^{(1)} = \begin{bmatrix} 1 & 0 & 0 \\ -1 & 1 & 0 \\ 0 & -1 & 1 \end{bmatrix}, \; C_{y_s}^{(3)} = \begin{bmatrix} 1 & 0 \\ -1 & 1 \end{bmatrix}, \tag{9}$$

$$C_{y_s}^{(2)} = \begin{bmatrix} 1 & 0 & 0 & 0 & 0 \\ -1 & 1 & 0 & 0 & 0 \\ 0 & -1 & 1 & 0 & 0 \\ 0 & 0 & -1 & 1 & 0 \\ 0 & 0 & 0 & -1 & 1 \end{bmatrix}. \tag{10}$$

Finally, the *inter-building approaches*

$$\{y_a\}_i^j = -\left(q_i^{j+1} - q_i^j\right), \; 1 \le i \le r_j, \; 1 \le j \le 2, \tag{11}$$

with $r_j = \min(n_j, n_{j+1})$, describe the approaching between the stories placed at the ith level in the adjacent buildings $\mathcal{B}^{(j)}$ and $\mathcal{B}^{(j+1)}$, which have a total number of stories n_j and n_{j+1}. The vector of inter-building approaches

$$y_a(t) = \left[\{y_a\}_1^1, \{y_a\}_2^1, \{y_a\}_3^1, \{y_a\}_1^2, \{y_a\}_2^2,\right]^T,$$

can be computed with the output matrix

$$C_{y_a} = \begin{bmatrix} I_3 & -[I_3]_{3\times 5} & [0]_{3\times 2} & [0]_{3\times 10} \\ [0]_{2\times 3} & [I_2]_{2\times 5} & -I_2 & [0]_{2\times 10} \end{bmatrix}. \tag{12}$$

To perform the numerical simulation of the seismic response corresponding to the different passive and active control configurations presented in the next sections, the following particular values for the building parameters have been used: m_i^j=1.29 $\times$ 10^6 kg, c_i^j=10^6 N s/m, k_i^1=2.4 $\times$ 10^9 N m, k_i^2=4 $\times$ 10^9 N m, k_i^3=2.4 $\times$ 10^9 N m, for $1 \le j \le 3$, $1 \le i \le n_j$, n_1=3, n_2=5, n_3=2. The linking elements are considered as pure

dampers with a damping constant $\hat{c}_i^j$=5 $\times$ 10^6 N s/m, and null stiffness; the value $\hat{c}_i^j$=0 indicates that no linking element exists at the ith level between buildings $\mathcal{B}^{(j)}$ and $\mathcal{B}^{(j+1)}$. In the active control strategies, it has been assumed that an ideal active bracing system has been placed between every two consecutive stories of the actively controlled buildings (see Fig. 7); the structure of the control placement matrices $T_u^{(j)}$ will be detailed in Section 4. Finally, a record of the North-South ground acceleration corresponding to El Centro 1940 earthquake (see Fig. 2) has been used as seismic excitation to simulate the vibrational response of the buildings.

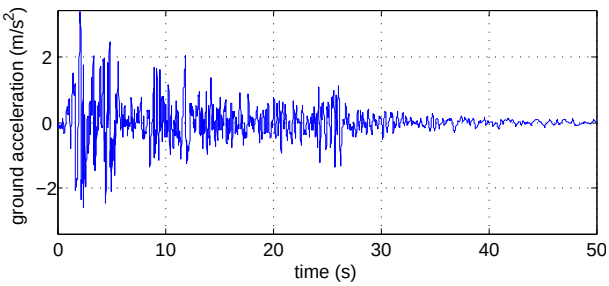

Figure 2. El Centro 1940 NS earthquake

3 PASSIVE LINKING CONFIGURATIONS

In this section, the seismic response of the three-building system for different configurations of the passive linking systems are studied and compared. For every passive control configuration, the overall control location matrix T_u is null; thus, the state-space model (6) takes now the form

$$\begin{cases} \dot{x}(t) = Ax(t) + Ew(t), \\ y(t) = C_y x(t). \end{cases} \tag{13}$$

The output matrix C_{y_s} given in (8), (9), (10) may be used to obtain the inter-story drifts, and the inter-building approaches can be computed with the output matrix C_{y_a} given in (12). Note that positive values of the inter-building approaches (11) indicate a reduction of the distance between the corresponding stories. It is clear that, in real-life situations, large values of the inter-building approaches may result in inter-building collisions. However, to keep the problem computationally tractable, the seismic response simulations will be conducted under the assumption that the inter-building separation is large enough to avoid collisions, and the maximum values of the inter-building approaches will be understood as lower bounds of *safe inter-building separation*.

Attending to the number and location of the linking devices, 32 different configurations of the linking system are possible, some of which are schematically displayed in Fig. 3 and Fig. 4. Case (a) corresponds to the uncoupled system; cases (b) and (c) are semi-coupled configurations; cases (d), (e), and (f) are full-coupled configurations of increasing complexity. Note that we use the term *semi-coupled* to indicate that only two of the buildings are linked, and the term *full-coupled* to point out that all the buildings are linked. The models corresponding to the different linking configurations are defined by the damping matrices (5). Thus, for example, the damping matrices for the

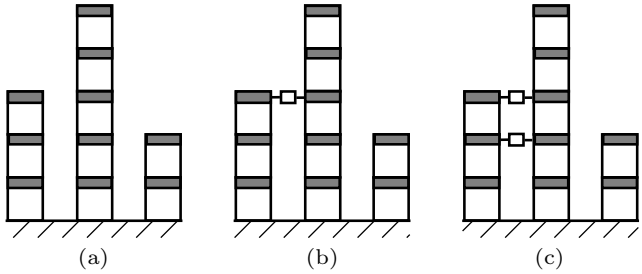

Figure 3. Passive linking configurations (I)

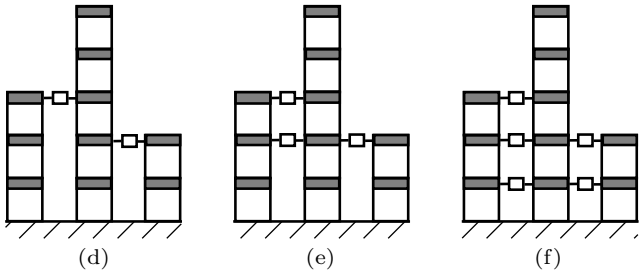

Figure 4. Passive linking configurations (II)

linking configuration (d) are

$$\hat{C}^{(1)} = \begin{bmatrix} 0 & 0 & 0 \\ 0 & 0 & 0 \\ 0 & 0 & 0.5\times 10^6 \end{bmatrix}, \hat{C}^{(2)} = \begin{bmatrix} 0 & 0 \\ 0 & 0.5\times 10^6 \end{bmatrix}. \tag{14}$$

Fig. 5 displays in blue squares the maximum absolute values of the inter-story drifts corresponding to the linking configuration (d); the red asterisks correspond to the uncoupled case (Subfig. 3-(a)). The graphics show clearly that the strategy of linking the buildings with damping devices at the top level has produced a seismic response reduction of about 50% with respect to the uncoupled system.

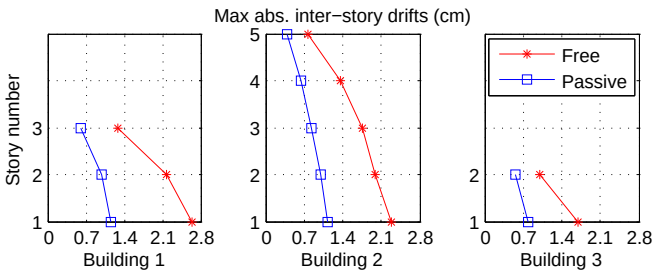

Figure 5. Maximum inter-story drifts for linking config. (d)

Looking at the maximum inter-building approaches displayed in Fig. 6, it can also be appreciated a significant reduction in the lower bounds of inter-building safe separation. For the uncoupled system (red asterisks), inter-building separations between buildings $\mathcal{B}^{(1)}$ and $\mathcal{B}^{(2)}$ inferior to 10 cm would have resulted in inter-building collisions; while separations slightly greater than 3 cm might be considered safe under the linking configuration (d) (blue squares).

For the linking configurations (b)–(e), the percentages of reduction in the maximum absolute inter-story drifts with respect to the uncoupled system are presented in Table 1; the

	Building 1			Building 2					Building 3	
	$\{y_s\}_1^1$	$\{y_s\}_2^1$	$\{y_s\}_3^1$	$\{y_s\}_1^2$	$\{y_s\}_2^2$	$\{y_s\}_3^2$	$\{y_s\}_4^2$	$\{y_s\}_5^2$	$\{y_s\}_1^3$	$\{y_s\}_2^3$
Link. config. (b)	56.9	53.6	51.1	41.4	40.1	42.9	41.1	39.2	0.0	0.0
Link. config. (c)	55.9	53.0	52.8	44.5	42.9	44.9	43.9	43.4	0.0	0.0
Link. config. (d)	56.8	54.8	53.1	50.9	49.9	52.9	52.0	49.6	53.4	45.5
Link. config. (e)	57.7	55.0	55.1	53.1	51.1	53.1	52.0	51.3	53.5	45.5
Link. config. (f)	57.0	55.9	55.9	53.7	51.4	53.3	52.3	51.9	57.1	51.2

Table 1. Reduction of maximum absolute inter-story drifts (%)

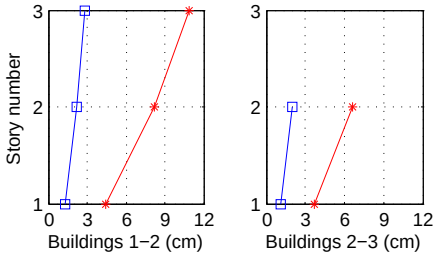

Figure 6. Max. inter-building approach. for linking config. (d)

corresponding percentages of reduction in the inter-building approaches are collected in Table 2. The data in the tables come to confirm the excellent results obtained by the linking configuration (d), with reductions of about 50% in the maximum absolute inter-story drifts and around 70% in the maximum inter-building approaches. The simulation data also reveal other interesting facts. Full-coupled configurations achieve a higher level of seismic protection than the semi-coupled ones. Linking systems consisting of a single damper placed at the top level may be considered optimal, in the sense that no significant increase in seismic protection results when more dampers are added. Unexpectedly, semi-coupled configurations provide some seismic protection to the uncoupled building; of course, there is no reduction of the inter-story drifts, but the reduction of the inter-building approaches is certainly remarkable.

	Buildings 1–2			Buildings 2–3	
	$\{y_a\}_1^1$	$\{y_a\}_2^1$	$\{y_a\}_3^1$	$\{y_a\}_1^2$	$\{y_a\}_2^2$
Link. config. (b)	67.9	68.3	69.3	43.9	44.7
Link. config. (c)	73.8	73.9	74.0	46.5	48.0
Link. config. (d)	71.1	72.8	73.8	69.7	70.1
Link. config. (e)	76.9	76.9	77.4	70.0	70.2
Link. config. (f)	78.2	78.4	78.7	72.1	72.0

Table 2. Reduction of maximum inter-building approaches (%)

4 PASSIVE-ACTIVE CONTROL CONFIGURATIONS

The aim of this section is to study the combined operation of passive damping inter-building control systems and local active control systems implemented in the buildings. We will suppose that the actively controlled buildings are equipped with ideal active bracing devices installed between every two consecutive

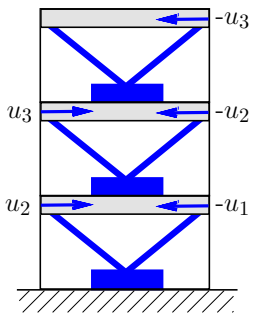

Figure 7. Active bracing system

stories as shown in Fig. 7; the actuation system will be driven by a local state-feedback LQR controller.

To compute a local state-feedback LQR controller for the actuation system in building $\mathcal{B}^{(j)}$, let us consider the local second-order model

$$M^{(j)}\ddot{q}^{(j)} + C^{(j)}\dot{q}^{(j)} + K^{(j)}q^{(j)} = T_u^{(j)}u^{(j)}, \tag{15}$$

where

$$q^{(j)} = \left[q_1^j, \ldots, q_{n_j}^j\right]^T$$

is the vector of story displacements relative to the ground,

$$u^{(j)} = \left[u_1^j, \ldots, u_{n_j}^j\right]^T$$

the vector of control forces, and n_j the number of stories; $M^{(j)}$, $C^{(j)}$, $K^{(j)}$ are, respectively, the local mass, damping, and stiffness matrix, which have been introduced in Section 2. The control location matrix $T_u^{(j)}$ has one of the following forms

$$T_u^{(1)} = \begin{bmatrix} -1 & 1 & 0 \\ 0 & -1 & 1 \\ 0 & 0 & -1 \end{bmatrix}, \quad T_u^{(3)} = \begin{bmatrix} -1 & 1 \\ 0 & -1 \end{bmatrix},$$

$$T_u^{(2)} = \begin{bmatrix} -1 & 1 & 0 & 0 & 0 \\ 0 & -1 & 1 & 0 & 0 \\ 0 & 0 & -1 & 1 & 0 \\ 0 & 0 & 0 & -1 & 1 \\ 0 & 0 & 0 & 0 & -1 \end{bmatrix}.$$

From (15), we obtain a first-order state-space model

$$\begin{cases} \dot{x}^{(j)} = A^{(j)}x^{(j)} + B^{(j)}u^{(j)}, \\ \{y_s\}^{(j)} = C_{y_s}^{(j)}x^{(j)}, \end{cases}$$

with local state vector

$$x^{(j)} = \begin{bmatrix} q^{(j)} \\ \dot{q}^{(j)} \end{bmatrix},$$

state matrix

$$A^{(j)} = \begin{bmatrix} [0]_{n_j} & I_{n_j} \\ -\{M^{(j)}\}^{-1}K^{(j)} & -\{M^{(j)}\}^{-1}C^{(j)} \end{bmatrix},$$

and control input matrix

$$B^{(j)} = \begin{bmatrix} [0]_{n_j} \\ \{M^{(j)}\}^{-1}T_u^{(j)} \end{bmatrix}.$$

To obtain the vector of inter-story drifts

$$\{y_s\}^{(j)} = \left[\{y_s\}_1^j, \ldots, \{y_s\}_{n_j}^j\right]^T,$$

we use the output matrix $C_{y_s}^{(j)}$, which has one of the forms given in (9), (10). We also take the weighting matrices

$$Q^{(j)} = \{C_{y_s}^{(j)}\}^T C_{y_s}^{(j)}, \quad R^{(j)} = 10^{-18.5} \times I_{n_j},$$

to define the quadratic cost function

$$\begin{aligned} J^{(j)}(x,u) &= \int_0^\infty \left[\{x^{(j)}\}^T Q^{(j)} x^{(j)} + \{u^{(j)}\}^T R^{(j)} u^{(j)}\right] dt, \\ &= \int_0^\infty \left[\{y_s^{(j)}\}^T y_s^{(j)} + \{u^{(j)}\}^T R^{(j)} u^{(j)}\right] dt. \end{aligned}$$

The resulting local LQR control matrices are

$$G^{(1)} = 10^8 \times \begin{bmatrix} -5.8702 & 0.0000 & 0.0000 & -0.3380 & -0.1509 & -0.1173 \\ 5.8702 & -5.8702 & 0.0000 & 0.1871 & -0.3044 & -0.1509 \\ 0.0000 & 5.8702 & -5.8702 & 0.0336 & 0.1871 & -0.3380 \end{bmatrix},$$

$$G^{(2)} = 10^8 \times$$

$$\begin{bmatrix} -3.7747 & 0.0000 & 0.0000 & 0.0000 & 0.0000 & -0.2666 & -0.1116 & -0.0770 & -0.0633 & -0.0579 \\ 3.7747 & -3.7747 & 0.0000 & 0.0000 & 0.0000 & 0.1550 & -0.2321 & -0.0979 & -0.0717 & -0.0633 \\ 0.0000 & 3.7747 & -3.7747 & 0.0000 & 0.0000 & 0.0346 & 0.1688 & -0.2267 & -0.0979 & -0.0770 \\ 0.0000 & 0.0000 & 3.7747 & -3.7747 & 0.0000 & 0.0138 & 0.0399 & 0.1688 & -0.2321 & -0.1116 \\ 0.0000 & 0.0000 & 0.0000 & 3.7747 & -3.7747 & 0.0054 & 0.0138 & 0.0346 & 0.1550 & -0.2666 \end{bmatrix}$$

$$G^{(3)} = 10^8 \times \begin{bmatrix} -5.8702 & 0.0000 & -0.3471 & -0.1740 \\ 5.8702 & -5.8702 & 0.1730 & -0.3471 \end{bmatrix}.$$

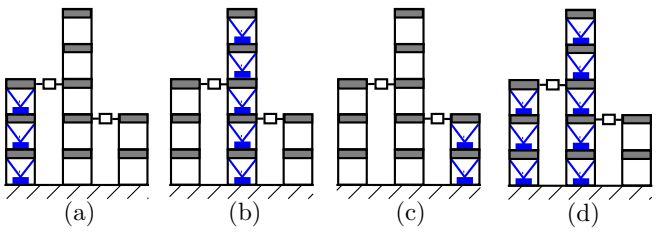

Figure 8. Passive-active control configurations (I)

The vector of control forces may be written as

$$u^{(j)} = G^{(j)} x^{(j)} = \left[\begin{array}{c|c} G_1^{(j)} & G_2^{(j)} \end{array}\right] \begin{bmatrix} q^{(j)} \\ \dot{q}^{(j)} \end{bmatrix},$$

where the matrices $G_1^{(j)}$ and $G_2^{(j)}$ are obtained by splitting the control matrix $G^{(j)}$ after the n_j-th column. The seismic response of the passive-active controlled systems can be simulated using the state-space model

$$\begin{cases} \dot{x} = \bar{A}x + Ew, \\ y = C_y x, \end{cases}$$

where the state matrix is $\bar{A} = A - BG$, the matrices B and E are given in (7), and the overall control matrix has the form

$$G = \left[\begin{array}{ccc|ccc} \bar{G}_1^{(1)} & [0]_{3\times5} & [0]_{3\times2} & \bar{G}_2^{(1)} & [0]_{3\times5} & [0]_{3\times2} \\ [0]_{5\times3} & \bar{G}_1^{(2)} & [0]_{5\times2} & [0]_{5\times3} & \bar{G}_2^{(2)} & [0]_{5\times2} \\ [0]_{2\times3} & [0]_{2\times5} & \bar{G}_1^{(3)} & [0]_{2\times3} & [0]_{2\times5} & \bar{G}_2^{(3)} \end{array}\right],$$

with

$$\bar{G}_i^{(j)} = \begin{cases} G_i^{(j)}, & \text{if } \mathcal{B}^{(j)} \text{ is actively controlled,} \\ [0]_{n_j}, & \text{otherwise.} \end{cases}$$

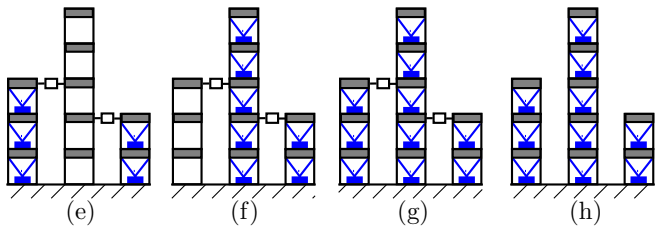

Figure 9. Passive-active control configurations (II)

Attending to the number and distribution of the actively controlled buildings, 8 different active control configurations are possible which, together with the 32 passive linking configurations, produce a total number of 256 different *passive-active control configurations* (PACCs). Note that the term PACC has been used in a broad sense, and may include non-active or decoupled configurations. Among the large number of PACCs, a set of 9 particular cases has been selected to illustrate the most salient features of the proposed passive-active control strategy. This testing set contains all the PACCs corresponding to the passive linking configuration (d), which has been chosen due to its balanced combination of simplicity and high performance. Plus, the decoupled full-active configuration has also been included to assess the possible interactions between the active and passive control systems.

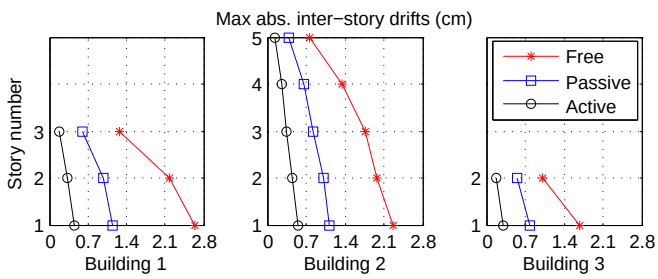

Figure 10. Max. abs. inter-story drifts for PACC (g)

A schematic representation of the passive linking configuration (d) can be seen in Subfig. 4-(d), while the remaining testing PACCs are displayed in Fig. 8 and Fig. 9; Subfig. 9-(h) corresponds to the decoupled full-active configuration. The

	Building 1			Building 2					Building 3	
	$\{y_s\}_1^1$	$\{y_s\}_2^1$	$\{y_s\}_3^1$	$\{y_s\}_1^2$	$\{y_s\}_2^2$	$\{y_s\}_3^2$	$\{y_s\}_4^2$	$\{y_s\}_5^2$	$\{y_s\}_1^3$	$\{y_s\}_2^3$
Passive config. (d)	56.8	54.8	53.1	50.9	49.2	52.9	52.0	49.6	53.4	45.5
Passive-Active config. (a)	83.7	86.2	86.3	51.0	50.9	55.3	56.6	53.2	53.0	45.1
Passive-Active config. (b)	57.1	58.0	58.2	76.0	77.1	78.5	78.9	80.1	51.9	43.3
Passive-Active config. (c)	56.9	54.9	53.2	50.2	48.8	52.7	50.3	47.1	82.5	82.3
Passive-Active config. (d)	82.7	85.4	86.2	75.8	77.0	79.1	79.3	80.4	51.7	43.3
Passive-Active config. (e)	83.8	86.3	86.4	50.4	50.4	55.3	54.2	50.6	82.4	82.2
Passive-Active config. (f)	57.3	58.0	58.2	76.0	77.1	79.4	79.7	80.9	81.9	82.1
Passive-Active config. (g)	82.7	85.5	86.3	75.8	77.0	80.0	80.2	81.2	81.9	82.1
Decoup. Active config. (h)	82.6	85.4	87.3	75.8	77.1	79.6	80.6	81.8	82.1	83.3

Table 3. Reduction of maximum absolute inter-story drifts (%) for passive-active control configurations

	Building 1			Building 2					Building 3	
	$\{y_s\}_1^1$	$\{y_s\}_2^1$	$\{y_s\}_3^1$	$\{y_s\}_1^2$	$\{y_s\}_2^2$	$\{y_s\}_3^2$	$\{y_s\}_4^2$	$\{y_s\}_5^2$	$\{y_s\}_1^3$	$\{y_s\}_2^3$
Passive config. (d)	0.00	0.00	0.00	0.00	0.00	0.00	0.00	0.00	0.00	0.00
Passive-Active config. (a)	7.80	6.29	3.60	0.00	0.00	0.00	0.00	0.00	0.0	0.0
Passive-Active config. (b)	0.00	0.00	0.00	9.85	9.13	8.02	5.90	3.18	0.00	0.00
Passive-Active config. (c)	0.00	0.00	0.00	0.00	0.00	0.00	0.00	0.00	5.41	3.30
Passive-Active config. (d)	7.99	6.44	3.69	9.71	9.00	7.85	5.88	3.16	0.00	0.00
Passive-Active config. (e)	7.79	6.28	3.60	0.00	0.00	0.00	0.00	0.00	5.43	3.32
Passive-Active config. (f)	0.00	0.00	0.00	9.67	9.01	7.89	5.82	3.14	5.45	3.32
Passive-Active config. (g)	7.98	6.43	3.68	9.54	8.86	7.72	5.80	3.11	5.45	3.32
Decoup. Active config. (h)	7.95	6.40	3.63	9.64	8.95	7.73	5.77	3.09	5.39	3.23

Table 4. Maximum control efforts for passive-active control configurations ($\times 10^6$ N)

percentages of reduction in the maximum absolute inter-story drifts achieved by the different testing PACCs are presented in Table 3, the corresponding percentages of reduction in the maximum inter-building approaches are collected in Table 5, and the maximum absolute control efforts are given in Table 4. In all the cases, the percentages have been computed with respect to the response of the *free system* (uncoupled and no actively controlled configuration (see Subfig. 3-(a)).

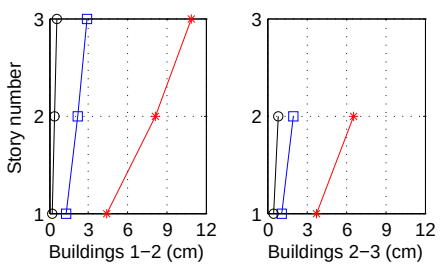

Figure 11. Max. inter-building approaches for PACC (g)

To get a more intuitive view, the behavior of the coupled and full actively controlled PACC (g) (see Subfig. 9-(g)) has been displayed in Fig. 10, Fig. 11, and Fig. 12. In these figures, the black circles represent the data corresponding to the PACC (g), the blue squares show the response of the passive linking configuration (d) (see Subfig. 4-(d)), and the red asterisks present the response corresponding to the free system. A quick

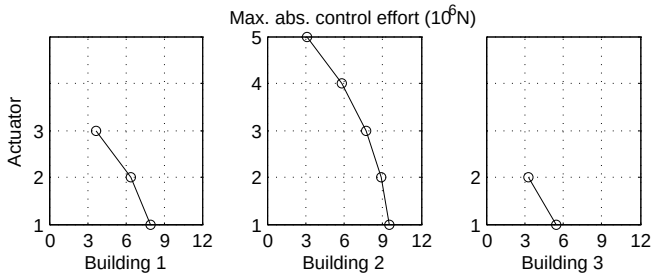

Figure 12. Max. control efforts for PACC (g)

look at the graphics clearly reveals the superior performance of the passive-active control system with respect to the pure passive linking system; however, these excellent results should be considered in light of the high complexity and large force requirements of the active control system, which would make it suitable only for cases where a high level of seismic protection is of critical importance.

A closer look at the data in Table 3 shows that the implementation of local active control systems increases significantly the percentages of reduction in the inter-story drifts from around the 50%, guaranteed by the passive linking configuration, to about 80%. Moreover, the behavior of the actively controlled buildings is practically independent on whether the neighboring buildings are actively controlled or not.

	Buildings 1–2			Buildings 2–3	
	$\{y_a\}_1^1$	$\{y_a\}_2^1$	$\{y_a\}_3^1$	$\{y_a\}_1^2$	$\{y_a\}_2^2$
Passive config. (d)	71.1	72.8	73.8	69.7	70.0
Pass.-Activ. config. (a)	83.2	82.5	81.4	69.6	70.1
Pass.-Activ. config. (b)	80.5	82.5	84.3	75.5	75.8
Pass.-Activ. config. (c)	70.7	72.5	73.6	74.0	71.6
Pass.-Activ. config. (d)	95.3	95.3	94.9	75.8	76.1
Pass.-Activ. config. (e)	83.1	82.4	81.3	74.1	72.2
Pass.-Activ. config. (f)	80.8	82.4	84.3	87.7	86.9
Pass.-Activ. config. (g)	95.0	95.1	94.8	88.1	87.4
Decoup. Act. conf. (h)	93.6	93.6	93.4	86.7	85.9

Table 5. Reduction of maximum inter-building approaches (%)

Regarding to the inter-building approaches, the data in Table 5 show that the implementation of local active control systems produces a moderate improvement in the percentages of reduction which, in this case, depend on the control configuration of the neighboring buildings. More precisely, for the inter-buildings approaches between $\mathcal{B}^{(1)}$ and $\mathcal{B}^{(2)}$, the 70% of reduction achieved by the passive linking configuration increases to about 80% when one of the buildings is actively controlled, and to around 90% when both buildings are under active control. For the inter-building approaches between $\mathcal{B}^{(2)}$ and $\mathcal{B}^{(3)}$, the percentage of reduction achieved by the passive linking configuration is also about 70%, this value increases slightly when one of the buildings is actively controlled, and more remarkably (to about 87%) when both buildings are under active control.

Finally, the values presented in Table 4 indicate that the maximum control effort required by a local active control system is practically independent of the active control configuration implemented in other buildings. Furthermore, the data corresponding to the decoupled full-active configuration displayed in the last row of the three tables show that the effect of the passive links on the local controllers performance is certainly small.

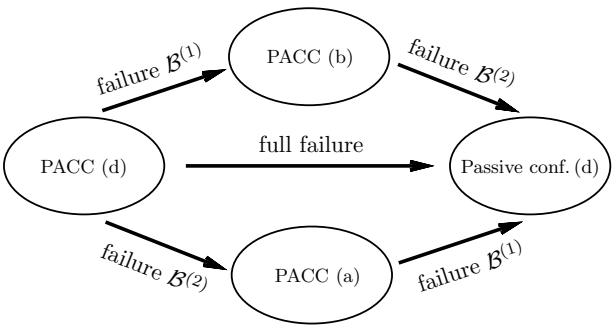

Figure 13. Failure diagram for PACC (d)

The obtained results can be seen from two interesting points of view. First, from the perspective of control design, the proposed passive-active approach provides a large and varied set of control configurations with different levels of complexity and seismic protection. Second, in the context of control reliability, any passive-active configuration has a set of associated PACCs which can be seen as its *failure modes*. When any of the local active control systems in a PACC fails, the overall control system shifts to a new PACC in its associated failure set, experiencing only a partial performance degradation. To illustrate these ideas, let us suppose that the PACC (d) (see Subfig. 8-(d)) has been chosen for a three-building system with buildings $\mathcal{B}^{(1)}$ and $\mathcal{B}^{(2)}$ requiring special seismic protection; then, the diagram in Fig. 13 displays the associated failure set and failure transitions.

5 CONCLUSIONS

A combination of active and passive control elements has been used to design a variety of control configurations to mitigate the seismic response of a three-building system. Numerical simulations have been carried out to assess the performance of the proposed methodology. The simulation results point out that a significant reduction in the inter-story drifts and the inter-building approaches of adjacent buildings under seismic excitation may be achieved by an adequate linkage of the adjacent buildings by means of passive dampers. In buildings which require a particularly high level of seismic protection, an additional local active control system may be implemented. The passive linking system has no adverse effect on the performance of the local active control systems; moreover, it guarantees a remarkable level of seismic protection in case of failure of any of the local active control systems.

ACKNOWLEDGMENTS

This work was supported in part by the Spanish Ministry of Science and Innovation and FEDER funds from the European Union through the grants DPI2008-06699-C02-02 and DPI2008-06564-C02-02.

REFERENCES

[1] S.A. Anagnostopoulos. Building pounding re-examined: How serious a problem is it? In *Eleventh World Conference of Earthquake Engineering*, number Paper No 2108. Elsevier Science ltd, 1996.

[2] S.D. Bharti, S.M. Dumne, and M.K. Shrimali. Seismic response analysis of adjacent buildings connected with magnetorheological dampers. *Engineering Structures*, (32):2122–2133, 2010.

[3] A.V. Bhaskararao and R.S. Jangid. Seismic response of adjacent buildings connected with friction dampers. *Bulletin of Earthquake Engineering*, 4:43–64, 2006.

[4] R.E. Christenson, B.F. Spencer, and E.A. Johnson. Semiactive connected control method for adjacent multidegree-of-freedom buildings. *Journal of Engineering Mechanics*, 133(3):290–298, 2007.

[5] G.W. Housner, L.A. Bergman, T.K. Caughey, and A.G. Chassiakos. Structural control: Past, present, and future. *Journal of Engineering Mechanics*, 123(9):897–971, September 1997.

[6] D. Lopez-Garcia and T.T. Soong. Assessment of the separation necessay to prevent seismic pounding between structural systems. *Probabilistic Engineering Mechanics*, (24):210–223, 2009.

[7] A. Preumont and K. Seto. *Active Control of Structures*. Wiley, United Kingdom, 2008.

[8] K. Seto, Y. Toba, and Y. Matsumoto. Reduced order modelling and vibration control methods for flexible structures arranged in parallel. In *Proceedings of the American Control Conference*, pages 2344–2348, Seattle, USA, 1995.

[9] B.F. Spencer and S. Nagarajaiah. State of the art of structural control. *Journal of Structural Engineering*, 129(7):845–856, July 2003.

[10] Z. Yang, Y.L. Xu, and X.L. Lu. Experimental seismic study of adjacent buildings with fluid dampers. *Journal of Structural Engineering*, 129(2):197–205, 2003.

[11] W.S. Zhang and Y.L. Xu. Dynamic characteristics and seismic response of adjacent buildings linked by discrete dampers. *Earthquake Engineering and Structural Dynamics*, 28:1163–1185, 1999.